NURETH14-472

CHECK VALVE SLAM CAUSED BY AIR INTRUSION IN EMERGENCY COOLING WATER SYSTEM

C. Samuel Martin
Georgia Institute of Technology, Atlanta, Georgia, U.S.A.
csammartin@comcast.net, smartin@ce.gatech.edu

Abstract

Waterhammer pressures were experienced during periodic starting of Residual Heat Removal (RHR) pumps at a nuclear plant. Prior to an analytical investigation careful analysis performed by plant engineers indicated that the spring effect of entrapped air in a heat exchanger resulted in water hammer due to check valve slam following flow reversal. In order to determine in more detail the values of pertinent parameters controlling this water hammer a hydraulic transient analysis was performed of the RHR piping system, including essential elements such as the pump, check valve, and heat exchanger. Using characteristic torque and pressure loss curves the motion of the check valve was determined. By comparing output of the water hammer analysis with site recordings of pump discharge pressure the computer model was calibrated, allowing for a realistic estimate of the quantity of entrapped air in the heat exchanger.

1. Introduction

Although the piping system for the RHR emergency cooling water system is actually somewhat more complicated, Figure 1 is presented to illustrate the essential features of the hydraulic system. The outside storage tank supplies the water to the RHR pump, which has a swing check valve on its discharge. After some 118 m of 200-mm piping there is an inverted U-Tube heat exchanger, which was suspected to contain entrapped air. For the situation at hand the piping terminates at the isolation valve to the reactor coolant system (RCS). Except for a minimum (MiniFlow) line not shown on Figure 1, there should be no flow in this dead-headed piping inasmuch as the RCS is isolated from RHR.

Inspection of the pressure recording taken during periodic startup of a RHR pump suggested that the measured water hammer spike was caused by rapid check valve closure (slam) due to flow reversal. It was suspected that air was trapped in the upper portions of the U-tubes in the heat exchanger. Once the air is compressed it acts like a spring, forcing water back through the check valves and pump. In order to simulate water hammer due to check valve slam modeling of the check valve response is essential. Although the recorded peak pressure was only up to 4 bar, analysis was conducted to (1) calibrate computational model, and (2) determine the possible maximum pressure for various assumed air volumes.

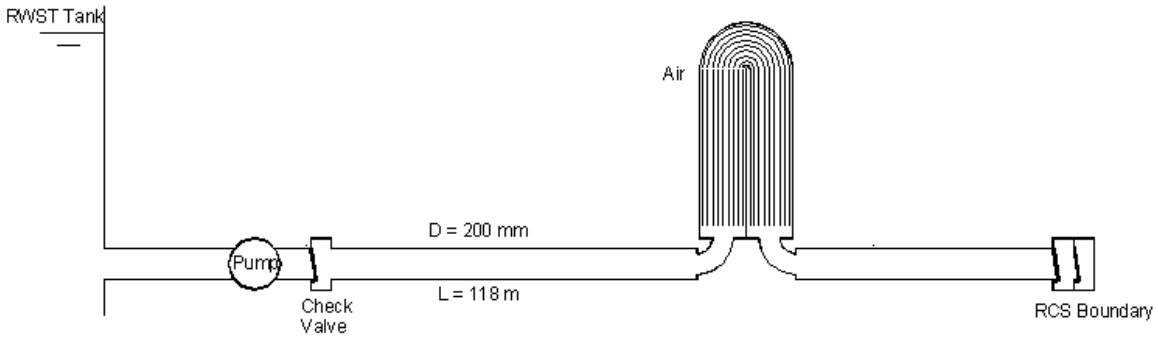

Figure 1 Schematic illustrating tank, piping, pump, check valve, and heat exchanger

2. Check valve dynamics

For all numerical simulations a swing check valves at pump discharge was dynamically simulated. Figure 2 provides a definition sketch of the swing check valve and its geometric characteristics.

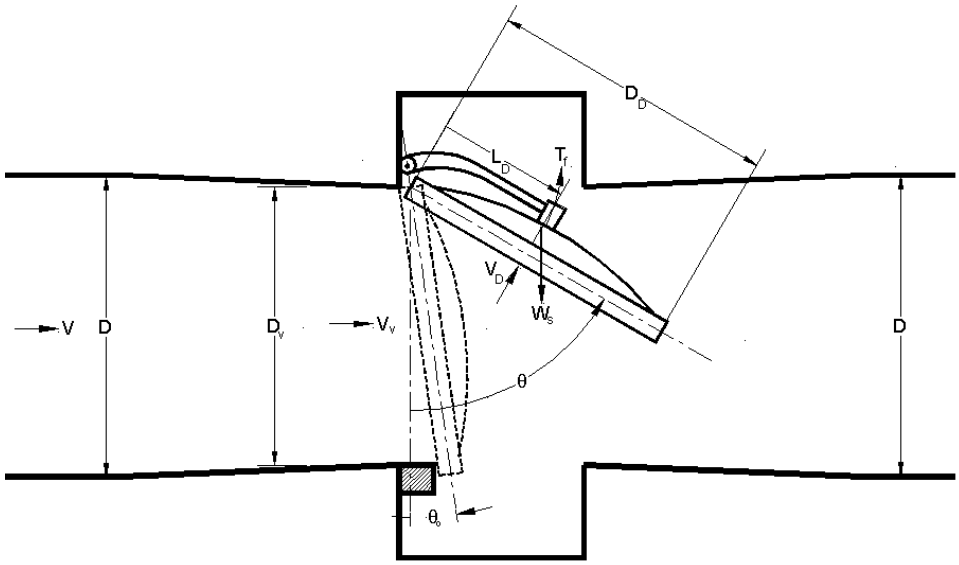

Figure 2 Diagram of check valve and definition of physical quantities

The following nomenclature defines the geometric and other features of the valve analysis.

L_D = Lever arm from pivot point to center of mass of valve disk, arm and other mechanisms
D_D = Diameter of valve disk
D_v = Diameter of valve opening
D = Diameter of pipe
V_v = Velocity through valve opening

$V_D = L_D d\theta/dt$ = Velocity of center of disk mechanism

V_R = Relative velocity between V_v and component of V_D

V = Velocity in pipe

W_s = Submerged weight of valve disk, arm and other mechanisms

$M_v R^2$ = Polar moment of inertia of submerged valve disk, arm and other mechanisms

T = Torque about pivot point

T_f = Fluid torque on valve disk

θ = Valve disk angle

θ_M = Maximum valve disk angle (58°)

For dynamic simulation of check valve response to transient flow, hydraulic characteristics are required. In addition to pressure-drop or head loss characteristics, dynamic simulation also requires information about the unbalanced torque on the valve disc in order to predict the valve position. Only a limited number of laboratory test results conducted under steady-flow conditions are available in the open literature. Some of these involve only measurement of pressure drop with the valve disc held at a fixed position. The results are usually correlated in terms of a head-loss coefficient K_L, Martin [1]

$$H_L = K_L \frac{V^2}{2g} \tag{1}$$

More comprehensive tests include the measurement of fluid torque at each position for varying flow rates. The fluid torque T_f can be correlated in terms of a torque coefficient C_M, defined by

$$T_f = C_M D^3 \frac{\rho V^2}{2} \tag{2}$$

By applying the angular momentum equations to the center of rotation, any torque, whether hydraulic, mechanical, or otherwise, can be incorporated.

$$\Sigma T = M_v R^2 \frac{d^2\theta}{dt^2} \tag{3}$$

Equation (3) equates the sum of torques to the angular acceleration, with the total rotating moment of inertia embodied in $M_v R^2$. The inertia term $M_v R^2$ includes that of the valve disc and arm, and added mass of the disc.

$$V_R = V_v - L_D \cos\theta \frac{d\theta}{dt} = \frac{VA}{A_v} - L_D \cos\theta \frac{d\theta}{dt} \tag{4}$$

For this analysis ΣT includes the fluid torque T_f and the torque due to the submerged weight W_s of the valve disc and arm, which reflects buoyancy force. Using Equation (2) for fluid torque, the angular acceleration of the check valve can be expressed in terms of the relative velocity of the center of mass of the valve assembly. It should be mentioned that bearing friction and damping were neglected in this analysis.

$$\frac{d^2\theta}{dt^2} = \frac{1}{M_v R^2}\left[C_M D^3 \frac{\rho V_R |V_R|}{2} - W_s L_D \sin\theta\right] \tag{5}$$

Kalsi [2] reports head-loss data for a 75-mm diameter swing valve. Measurements of head loss and fluid torque are reported by Nece and Dubois [3] for a 150-mm swing check valve. Later tests were reported by Kane and Cho [4] for a 400-mm tilting disc check valve. Head loss coefficient K_L and torque coefficient C_M curves representative of the three valves are illustrated by Figure 3. As expected, both coefficients approach very high values for small valve disk angles θ.

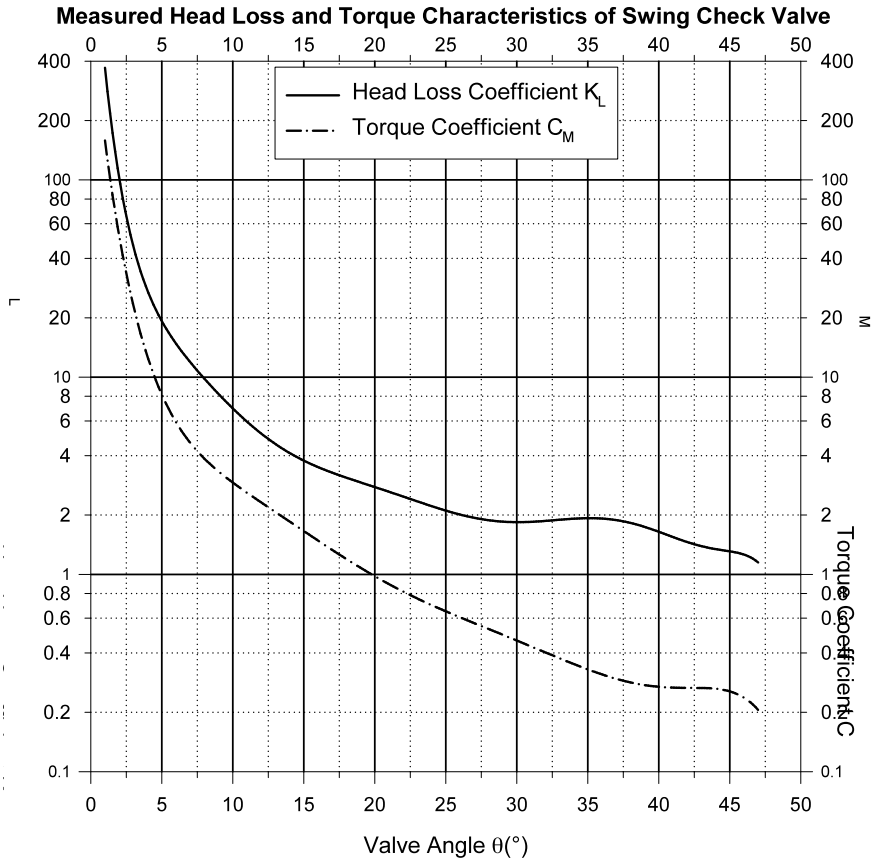

Figure 3 Coefficients of head loss K_L and torque C_M for swing check valve

3. Heat exchanger

The heat exchanger is a four-pass inverted U-tube type with 375 16.56 mm internal diameter tubes in each pass. In order to incorporate any entrapped air in the U portion of the tubes, each pass of tubes was represented by two runs, each 5.64 m in length. A cross section of 375 tubes was replaced by an equivalent tube of the same area, which corresponds to a diameter of 320 mm. In order to incorporate the same fluid friction using Darcy-Weisbach equation, an equivalent resistance coefficient was calculated; that is, f = 0.712 versus 0.026 for a single tube.

4. Pump

The head-discharge and power-discharge characteristics of the RHR pump as supplied by the manufacturer were employed. The rated point for the pumps corresponded to Q = 0.190 m^3/s (flow), H = 120 m (head), P = 280 kW (power), and e = 80% (efficiency). The best-efficiency or optimum point occurs at Q = 0.284 m^3/s and H = 99 m. The characteristics of the pump were incorporated into the water hammer analysis. Head-discharge and torque-discharge curves were reduced. The pump polar moment of inertia M_pR^2 = 2.03 kg•m^2.

5. Motor

For simulation of pump startup the torque-speed curve of the motor is required once the unit is energized. The torque-speed curve provided by the motor manufacturer was utilized. The manufacturer's curve shown in Figure 4 in terms of percentage of motor torque (rated T = 1,600 N•m) versus percentage rotational speed at 100% voltage.

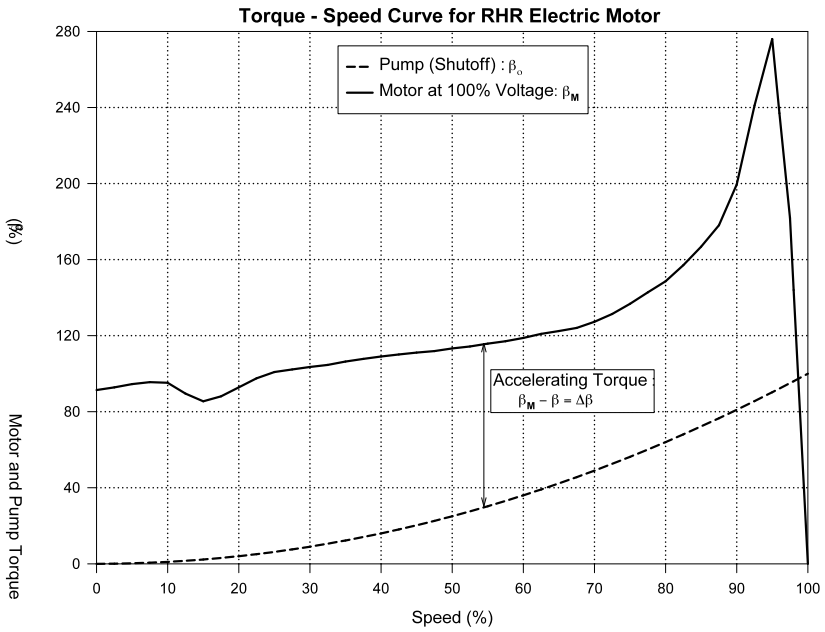

Figure 4 Torque-speed curve for motor

The unbalanced or accelerating torque is the difference between that supplied by the motor and that resisted by the pump. The lower curve in Figure 4 would only be the case if there were no flow; that is, the pump starting against a closed valve. For this analysis the pump torque was evaluated every time step by knowing the instantaneous pump flow and motor speed. The polar moment of inertia for the motor itself is 5.72 kg•m^2 , resulting in combined pump and motor assembly inertia of 7.75 kg•m^2. The time to accelerate the pumps and motors to full speed of 1780 rpm depends upon the starting voltage as well as the inertia (M_pR^2) of the rotating parts.

6. Method of analysis

For the hydraulic transient analysis the well-accepted technique of water hammer analysis, the method of characteristics (MOC), was employed. Details regarding development of MOC and its usage are provided in Wylie and Streeter [5] and Chaudhry [6]. The computer program entitled PNET was utilized, which is a comprehensive coded water hammer program based upon MOC.

Equation (3) equates the sum of torques to the angular acceleration, with the total rotating moment of inertia embodied in M_vR^2. The inertia term M_vR^2 includes that of the valve disc and arm, and added mass of the disc. For this analysis ΣT is the fluid torque T_f and the torque due to the submerged weight W_s of the valve disc and arm. Using Equation (2) for fluid torque, the angular acceleration of the check valve can be expressed in terms of the relative velocity of the center of mass of the valve assembly. At each time step Equation (5) is solved numerically utilizing Runge-Kutta. Knowing the valve angle θ the velocity V in the pipe is determined by MOC, which uses the head-loss coefficient from Figure 3 to calculate the pressure drop across the valve. For each pipe the wave propagation speed was computed using the standard equation. When necessary the wave speed was modified to satisfy the Courant criterion so that the time step for each computer pipe was identical. The initial conditions are relatively simple inasmuch as there is no flow. The transient was initiated by energizing the motor connected to the RHR Pump.

7. Effect of air in heat exchanger

Once the piping system and its components were coded effort was expended to calibrate PNET output with site recordings. It was discovered that the principal variable was the volume of air in the heat exchanger. By varying the entrapped air volume from 0 to 750 liters the amount of air necessary to mimic the pressure recording near pump discharge was determined.

For purposes of comparison, an analysis representing no entrapped air, was also simulated. The time-history results are plotted in Figure 5. The top trace, which is virtually independent of air, show the motor, which is made to start at T = 0.2 second, attained full rotational speed at approximately T = 1.0 second, corresponding to an acceleration time of 0.8 second. The check valve disc, which is at an angle $\theta = 8°$ when closed, begins to open at T = 0.6 second. Even though there is no air in the heat exchanger, the compressibility of the water within the entire loop and the added elasticity of the piping caused a flow difference between the pump and the MiniFlow line. The flow suddenly peaks at about 0.025 m^3/s, slightly below the final steady-state flow of 0.032 m^3/s through the MiniFlow line. The peak heat exchanger pressure for the no air simulation is 1.94 Mpag, occurring at T = 1.28 seconds.

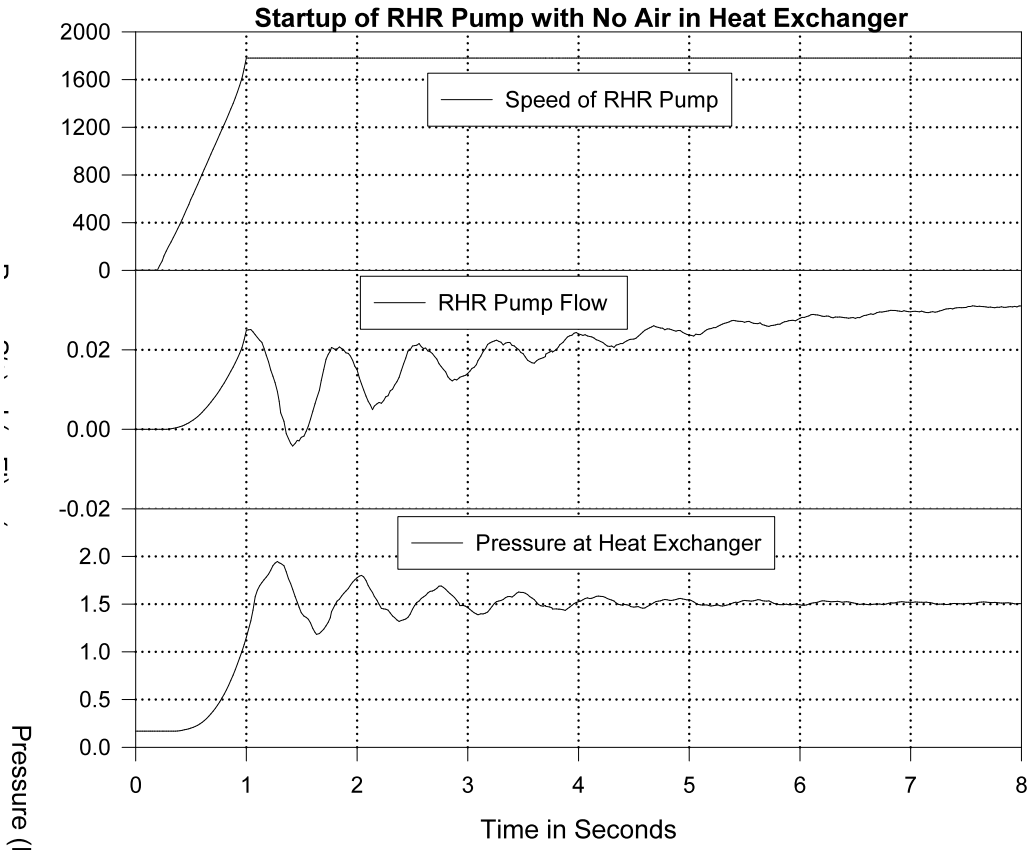

Figure 5 Simulation of pump startup with no air in heat exchanger

Figure 6 shows the computed time histories for an initial air volume of 475 liters. Because of the increased flow directed toward the heat exchanger, the check valve opens to its full position of $\theta = 58°$ at T = 0.96 second. Note that the pump flow peaked at 0.230 m^3/s at approximately 2.06 seconds, then commenced deceleration. As the flow rate drops, the check valve can no longer be maintained at $\theta = 58°$, beginning to close at T = 3.41 seconds. At pump discharge there is an initial pressure peak at the instant the motor attained full speed (T = 1.0 second). The flow continues to accelerate for this time, yielding maximum pressure at the heat exchanger at 3.4 seconds, the time of zero flow. This peak pressure of 2.75 Mpag is due to entrapped air alone. After flow reversal at T = 3.5 seconds, check valve slam occurs at T = 3.74 seconds, resulting in a peak pressure of 4.1 Mpag.

For air volumes from 95 to 475 liters, the time histories shown on Figure 7 are similar, but the times are increased due to the increased cushioning of the air effect. Clearly, as the entrapped air volume is increased the effect of flow reversal is minimized, yielding reduced effect of check valve slam.

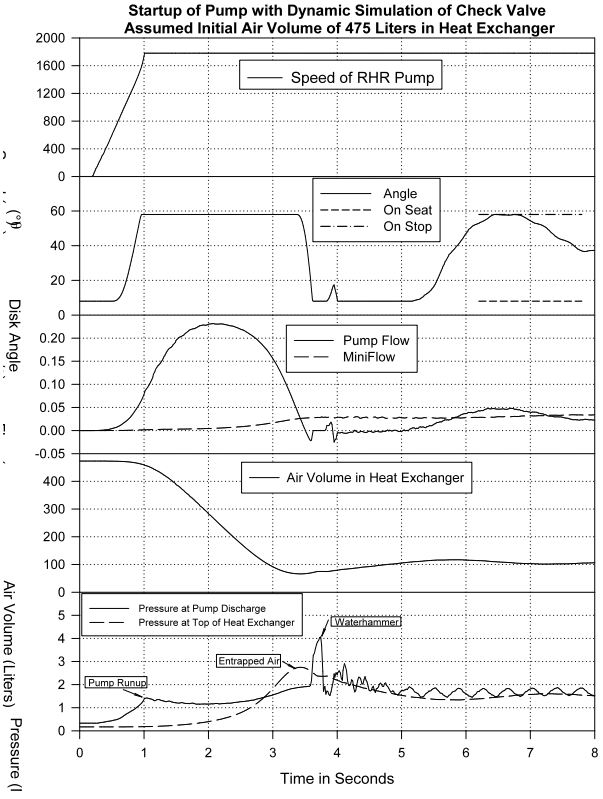

Figure 6 Simulation of check-valve slam with air

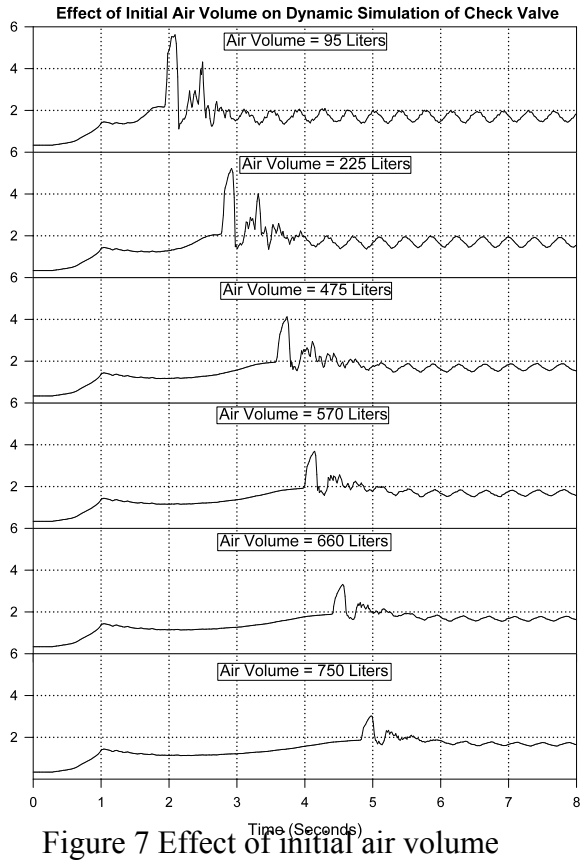

Figure 7 Effect of initial air volume

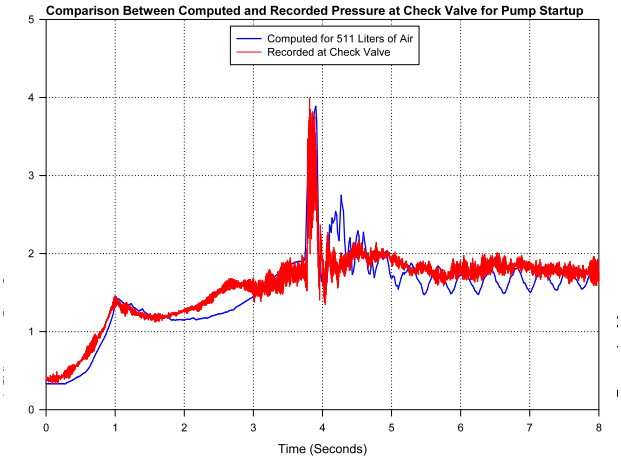

Figure 8 Pressure recording versus analysis

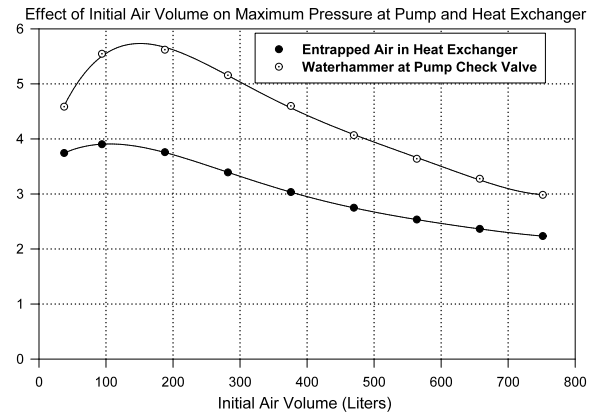

Figure 9 Effect of air volume on pressure

The main purpose of these analyses was the calibration of PNET against a plant recording, so that additional computations can be accomplished to ascertain the effect of surge protection and other fixes. For the periodic test conducted the closest fit between PNET output and plant recording occurred for an initial air volume of 511 liters, as shown by the two traces on Figure 8. The effect of initial air volume on the peak waterhammer pressure is shown by the data on

Figure 9. Figure 10 shows the effect of initial air volume on the time of check-valve slam, as derived from the results on Figure 9. Another indicator of check valve response is the deceleration of the water column, denoted by dV/dt. For air volumes 95 liters and higher Figure 11 shows that this quantity gradually decreases.

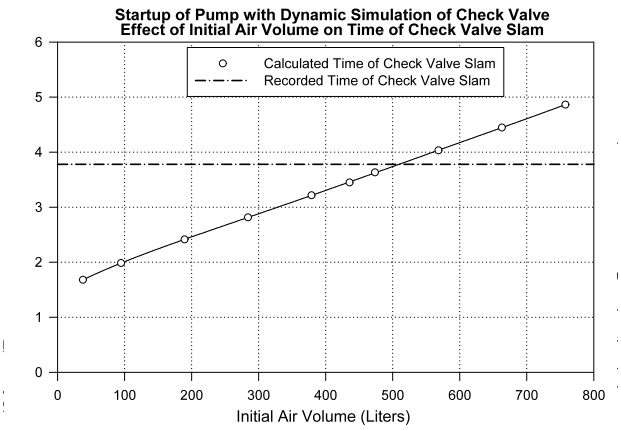

Figure 10 Effect of air on deceleration time

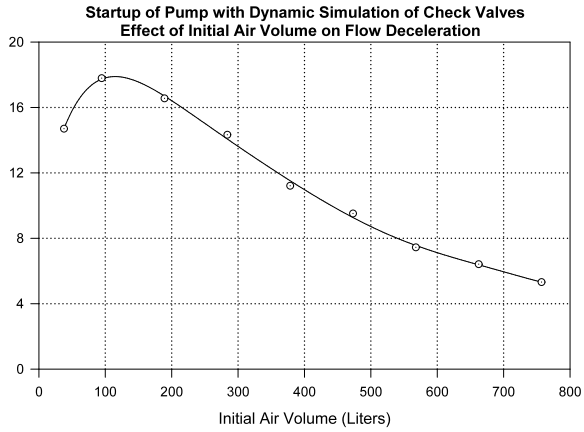

Figure 11 Effect of air on deceleration

Check valve dynamics can also be related to piping system characteristics; namely, the value of flow deceleration, as summarized by Wylie and Streeter [5]. In fact, many analysts prefer the correlation of maximum reverse velocity through a check valve with the flow deceleration dV/dt. Although this method of analysis was not employed in this investigation, the output of results illustrates the same correlation of maximum reverse velocity through check valve with dV/dt, as shown on Figure 12.

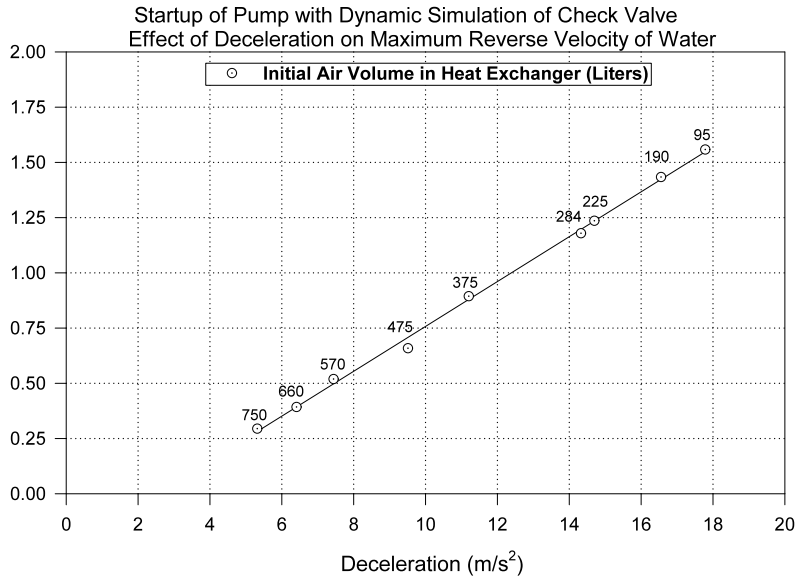

Figure 12 Effect of deceleration on maximum reverse velocity

8. Summary

Computer analysis was able to closely reproduce a plant recording of pump startup of an RHR pump, confirming that the waterhammer experienced was caused by entrapped air, followed by check valve slam. It has been demonstrated that the presence of air in a heat exchanger coupled with slow response of a swing check valve causes waterhammer due to flow reversal and check valve slamming, and is in good agreement with plant recording if the initial air volume is 511 liters.

The computer analysis matches not only the peak pressure, but also the time of occurrence relative to pump startup. The effect of initial air volume on both the maximum transient pump flow and the peak waterhammer pressure was ascertained once the model was calibrated. The maximum waterhammer pressure was 5.6 Mpag for 151 liters of air.

Various solutions were contemplated to reduce the effect of entrapped air on unwanted pressure peaks; namely, two were:

a. Installation of an accumulator with much larger air volume.

b. Maintenance of pressure with jockey pump.

9. References

[1] Martin, C. S., "Hydraulics of Valves", Chapter 25.3, *Handbook of Fluid Machinery*, McGraw-Hill, 1996, pp. 2043-2067.

[2] Kalsi, M. S. and Horst, Todd, “Swing Check Valve Disk Stability Under Turbulence”, Combined ASME/ANS Nuclear Engineering Conference, Myrtle Beach, April 17-20, 1988.

[3] Nece, R.E. and Dubois, R.E., "Hydraulic Performance of Check and Control Valves," *Journal of the Boston Society of Civil Engineers*, Vol. 42, July, 1955, pp. 263-286.

[4] Kane, R. S. and Cho, S. M., "Hydraulic Performance of Tilting-Disc Check Valves,"*Journal of the Hydraulics Division*, ASCE, Vol. 102, HY1, January 1976, pp. 57-72.

[5] Wylie, E. B. and Streeter, V. L., *Fluid Transients in Systems*, Prentice-Hall, 1993.

[6] Chaudhry, M. H., *Applied Hydraulic Transients*, van Reinhold Nostrand, 1987.